Periodicals of Engineering and Natural Sciences ISSN 2303-4521
Vol. 9, No. 2, June 2021, pp.1073-1085

Quadtree partitioning scheme of color image based

Ghadah K. AL-Khafaji[1], Mohammed H. Rasheed[2], and Omar M. Salih[3]
[1]Dept. of Computer Science, College of Science, University of Baghdad, IRAQ
[2,3]Computer Engineering Dept., Technical College/Kirkuk, Northern Technical University, IRAQ

ABSTRACT

Abstract: Image segmentation is an essential complementary process in digital image processing and computer vision, but mostly utilizes simple segmentation techniques, such as fixed partitioning scheme and global thresholding techniques due to their simplicity and popularity, in spite of their inefficiency. This paper introduces a new split-merge segmentation process for a quadtree scheme of colour images, based on exploiting the spatial and spectral information embedded within the bands and between bands, respectively. The results show that this technique is efficient in terms of quality of segmentation and time, which can be used in standard techniques as alternative to a fixed partitioning scheme.

Keywords: Image Segmentation, Quadtree, DPCM, Spatial and Spectral Information

Corresponding Author:

Ghadah K. Al-Khafaji
Dept. of Computer Science, College of Science, University of Baghdad
Baghdad, Iraq
E-mail: ghada.toma@sc.uobaghdad.edu.iq

1. Introduction

The aim of image segmentation techniques is to separate (isolate) the significant foreground part (region of interest) from non-significant (non-region of interest) background parts, where each region hold its characteristics or features. The techniques for achieving efficient separation vary according to the way that gray level (intensity) values are utilized or exploited. This is basically classified into two groups, either of discontinuity (boundary) or similarity (continuity). The choice between the techniques is determined by the problem being considered. Background information related to the segmentation process can be found in [1-4]; for reviews of various image segmentation techniques see [5-12].

Split-merge of region-based segmentation techniques first appeared in the last century as a tool for coding (compression), and was adopted by Fisher [13] in his books as an experiment to encode the fractal by exploiting the partitioned iterated function system (PIFS) embedded, using the quadtree and HV (horizontal-vertical) schemes. Since then, a large number of works have been introduced to facilitate the process with further proposals of various homogeneity measures, adaption schemes and block shapes; for more details see [14-23].

Today, joint photographic expert group (JPEG) is the most well-known standard compression technique. It utilizes a fixed partitioning scheme. The question arises that if the split-merge techniques have proven their effectiveness, why have they not been incorporated into this standard techniques? In reality, the split-merge technique still suffers from certain problems, which can be summarized as the non-standardization of the model of homogeneity (uniformity), the shape nature of the block (quadtree, HV, triangular), and the partitioning time and computation required. Here we introduce a new quadtree partitioning scheme of color images, based on exploiting the spectral and spatial information. It is significantly useful in providing an efficient block-segmentation-based technique that is also fast. The paper organized as follows: section 2 is concerned with related work, section 3 discusses the proposed partitioning scheme, and finally sections 4 and 5 give the experimental tested results and the main conclusions.

2. Related work

As mentioned previously, Fisher [13] introduced the quadtree scheme as part of fractal coding, to utilize the same number of coefficients (i.e., scale, offset, symmetry) for homogenous regions of different sizes, namely partitioning of the image into different block sizes (n×m), according to the uniformity measure, and then model each region using the fractal parameters (i.e., 3 coefficients). The technique suffers from a long encoding time due to the matching between range/domain pools, since the partitioning process is implemented during the search for optimal coefficients estimation. This is not considered an efficient technique due to its time complexity. This section provides a survey of quadtree segmentation-based techniques using different uniformity measures and various adaptation scheme processes. Details of various different quadtree graphic data structures can be found in [24].
The efforts are concentrated on partitioning images hierarchically using variable block sizes of gray images. The early work included Jamila [17], which proposed a new quadtree partitioning method that did not depend on Fisher's methodology, but created the partitioned image independently from the searching (matching) process. The technique exploits the uniformity measure that utilizes the pixel value dispersion from the average brightness of each block. Here we have to mention some of the uniformity measures adopted, such as Ghadah [25], which adopted a statistical uniformity measure of mean and standard deviation along the control parameters of maximum/ minimum block size and threshold value. Zainab [26], utilized the boundary of the region along the geometric feature orientation of the moment of inertia as a measure of homogeneity to subdivide the region. Qaswaa and Haider [27], exploited the modelling principle as a measure of uniformity using the Sobel gradient residual of each block. Ghadah et. al. [28], used the fixed predictor scheme along the hierarchal uniformity measure of a statistical basis. The second part of this quadtree survey relates to the scheme adaptation or partitioning methodology, including Detlev et. al. [29], and Zhao et. al. [30], which adopted successive recursive subdivision, where each step partitioned into four equal sized quadrants. Other schemes have utilized merging approaches, where the is image partitioned or split into fixed regions (blocks), then according to a given threshold value the adjacent blocks are merged. This was adopted by Ghadah and Loay [31], and Philipp et. al. [32]. This scheme can also be extended more than once, in a layered fashion, as adopted by Rafiq et. al. [33]. Finally, other schemes of Weighted Finite Automata, searching and indexing, have been adopted by Chim and Kai [34] and Francesco et. al. [35], respectively.

3. Proposed system of quadtree partitioning scheme

Most of the work surveyed is concerned with gray-based images where a single band image is segmented using a quadtree scheme. In this paper we introduce a new color method of quadtree partitioning, using the spatial and spectral information efficiently. It depends on the embedded correlation between the color bands, and within each color band on a spatial (inter) basis. Figure (1) shows the proposed system using the RGB base. The color transformation base was not considered in order to reduce the spectral redundancy embedded between color space conversions. The steps below demonstrate the implementation:

1. Load the input color image I of size N×N, where I corresponds to an input image of three color bands (layers) of RGB base.
2. Separate the color image I into its bands, each of size N×N, where I is decomposed into I_R,I_G and I_B; these bands (layers) imply the spectral information or correlation information embedded between the color image bands.
3. Use the spectral color bands to find the first spectral threshold value using the cross correlation embedded between the color band and its average; in other words compute the cross correlation between each two correlated bands (i.e., I_RI_G, I_RI_B, I_GI_B), then find the average values between these computed cross-correlation color bands, according to the equations below [36-38]:

$$CoR(xband, yband) = \frac{\sum_{x=0}^{N-1} \sum_{y=0}^{N-1} Cov(xband, yband)}{\sqrt{Cov(xband, xband) \times Cov(yband, yband)}} \quad (1)$$

$$Cov(xband, yband) = \frac{1}{N^2} \sum_{i=1}^{N} \sum_{j=1}^{N} \left[(X_a(i,j) - M_a) - (X_b(i,j) - M_b) \right] \quad (2)$$

$$M_a = \frac{1}{N^2} \sum_{i=1}^{N} \sum_{j=1}^{N} X_a(i,j) \quad (3)$$

$$M_b = \frac{1}{N^2} \sum_{i=1}^{N} \sum_{j=1}^{N} X_b(i,j) \quad (4)$$

Where CoR(xband, yband) corresponds to the cross correlation of color image bands, Cov is the covariance, which measures the interaction between brightness values, M_a and M_b are the mean values of each color band of xband, yband respectively, N×N is the image size, and $X_a(i,j)$ and $X_b(i,j)$ are the pixel values of the image at location (i,j) in the color image xband and yband, respectively.

$$AvCoR = \frac{CoR(I_R, I_G) + CoR(I_R, I_B) + CoR(I_G, I_B)}{3} \quad (5)$$

Here the average cross correlation is represented by AvCoR. The cross correlation between the color bands corresponds to $CoR(I_R,I_G)$, $CoR(I_R,I_B)$ and $CoR(I_G,I_B)$.
The computed spectral threshold (Thr_{Spr}) equals:

$$Thr_{Spr} = AvCoR \times Factor_1 \quad (6)$$

Where $Factor_1$ is a determined spectral contribution value.

4. Use the separated color bands independently to find the second spatial threshold value using the modeling concept of each band separately, namely apply the differential pulse code modulation (DPCM) adopted for coding the Dc's values in JPEG [39], where it is applied to each band independently according to the equations below, then find the sum of absolute values of each one. Finally we compute the averaged between them, such that:

$$DPCM_{xband}(i,j) = DPCM_{xband}(i,j) - DPCM_{xband}(i+1,j) \quad (7)$$

$$Sp_{xband} = \frac{1}{N^2} \sum_{i=1}^{N} \sum_{j=1}^{N} abs(DPCM_{xband}(i,j)) \quad (8)$$

$$AvDPCM = \frac{Sp_{IR} + Sp_{IG} + Sp_{IB}}{3} \quad (9)$$

Where $DPCM_{xband}$ corresponds to the DPCM of each color band, Sp_{xband} is the sum of absolute values of DPCM of each color band (I_R,I_G, I_B) and AvDPCM is the average of the DPCM of the three bands.
The computed spatial threshold (Thr_{Spl}) equals to:

$$Thr_{Spl} = AvDPCM \times Factor_2 \quad (10)$$

Where $Factor_2$ is a determined spatial contribution value.

5. Determine or select the partitioning control parameters of maximum (M_{xb}) and minimum (M_{nb}) block sizes.
6. Partition the color image I into non-overlapped blocks of a quadtree scheme of variable sizes (n×m), using the spatial and spectral uniformity measure, such that:

a) Divide each color image separately (I_R,I_G,I_B) into fixed blocks of maximum sizes (i.e. $M_{xb}\times M_{xb}$).
b) Check the uniformity of the color bands blocks (I_R,I_G,I_B) using the spectral and spatial information regions, where if the blocks (regions) are non-uniform, partition the I color image into four quadrants until uniformity conditions are satisfied using the sub-steps below, or until the minimum block size is reached.

1) For each region of size $M_{xb}\times M_{xb}$ in each of the three bands (I_R,I_G,I_B), compute the mean and average them:

$$M_{bl} = \frac{1}{M_{xb}^{\;2}} \sum_{i=1}^{M_{xb}} \sum_{j=1}^{M_{xb}} X_{bl}(i,j) \qquad (11)$$

$$AvSpr = \frac{Mbl_{IR} + Mbl_{IG} + Mbl_{IB}}{3} \qquad (12)$$

Where M_{bl} is the computed mean block of size $M_{xb}\times M_{xb}$ of the three color separated bands (I_R,I_G,I_B), and AvSpr is the average of the three segmented blocks of the color bands Red, Green and Blue, respectively.

2) For each region of size $M_{xb}\times M_{xb}$ in each of the DPCM-based differentiated images of the three bands independently, compute the mean absolute DPCM of each block image and average them:

$$M_{bl}DPCM = \frac{1}{M_{xb}^{\;2}} \sum_{i=1}^{M_{xb}} \sum_{j=1}^{M_{xb}} abs(DPCMX_{bl}(i,j)) \qquad (13)$$

$$AvSpl = \frac{Mbl_{IR}DPCM + Mbl_{IG}DPCM + Mbl_{IB}DPCM}{3} \qquad (14)$$

Where $M_{bl}DPCM$ is the computed mean block of size $M_{xb}\times M_{xb}$ of the each of the differentiated images, and AvSpl is the average of the three segmented blocks of the color bands Red, Green and Blue respectively.

3) Check the uniformity condition of each block:
If (AvSpr > Thr_{Spr}) and (AvSpl > Thr_{Spl}) then non-uniform
Else uniform

The uniformity measure exploits the mean of the original color bands on a spectral basis, and the mean of the DPCM image on a spatial basis, where for a non-uniform region it exceeds certain spectral and spatial threshold values.

4) Test the segmented non-uniform blocks using the same steps as above, where the block size is equal to $M_{xb/2}\times M_{xb/2}$.

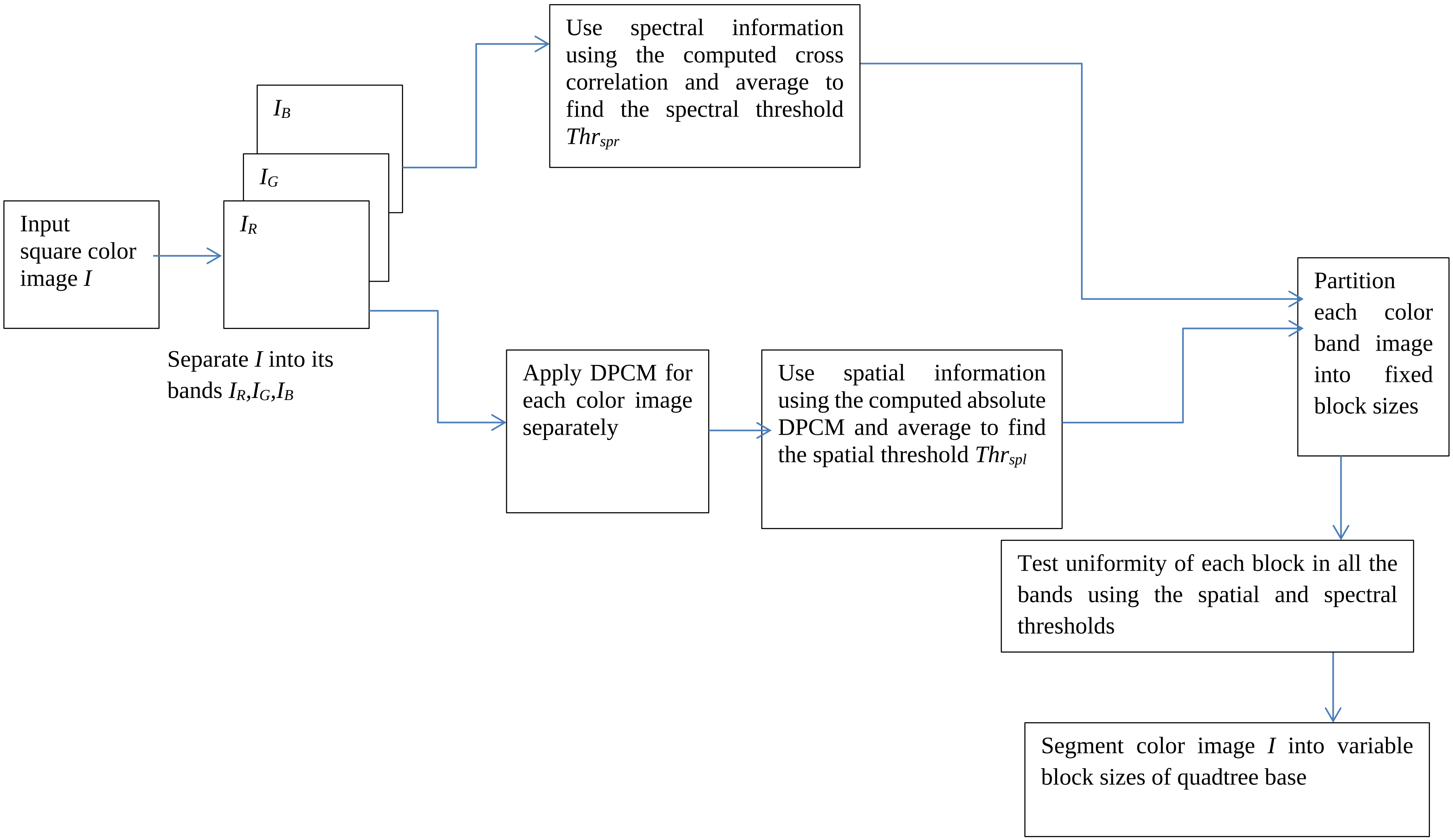

Figure 1. The proposed quadtree system of color images

4. Experimental results

The proposed system of color quadtree segmentation, utilizes four standard color square images of two sizes: 256×256 and 512×512 (see Figure (2)). The partitioning control parameters of maximum and minimum block sizes need to be selected (i.e., M_{xb}=16 and M_{nb}=2), and lastly $Factor_1$ and $Factor_2$ correspond to the contribution of spectral and spatial values used, such as (70,30) respectively, or other selected values (i.e., (60,40), (50,50), (80,20), always totalling 100). Figure (3) shows the color tested image bands of Figure (2), and Figure (4) shows the DPCM of the color bands of the tested images. The proposed system was implemented using Mathlab (R2008a) programming language, on a laptop computer with a processor intel(R) Core (TM) i5-2450CPU@2.50GHz, RAM 6.00 GB.

Figure 2. Tested color images of two sizes, where (a) Lena and (b) Pepper correspond to 512×512 images, (c) Girl and (d) House correspond to 256×256 images

Tables (1-2) demonstrate the computed cross correlation of spectral information and its average, the absolute difference of DPCM of each band and the average of the tested images, respectively. The results from the first table illustrates that the cross correlating, which is a measure of correlation embedded between color image bands, varies according to the ordering bands along the image details and characteristics. The second table demonstrates the fit of the DPCM base, where a small number means a good fit, and vice versa. Table (3) illustrates the computed spectral and spatial threshold values of the tested images using the $Factor_1$ and $Factor_2$ values, where the spatial and spectral threshold values are proportional to the values of the factors adopted; the higher the factor of values, the higher the threshold values, and vice versa.

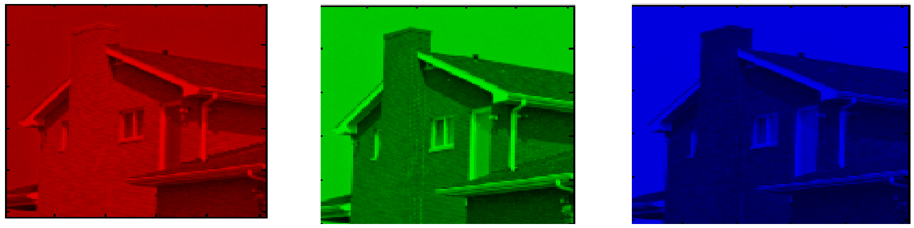

Figure 3. The red, green, and blue color bands of the tested images

Table 1. The cross-correlation between color image bands and its average for the tested images

Tested images	CoR(I_R,I_G)	CoR(I_R,I_B)	CoR(I_G,I_B)	AvCoR
Lena	0.9232	0.7718	0.9360	0.8770
Pepper	0.2752	0.3952	0.8379	0.5028
Girl	0.7712	0.6819	0.9126	0.7886
House	0.6378	0.4823	0.9418	0.6873

Table 2. The absolute error of DPCM of each color band and its average for the tested images

Tested images	Sp_R	Sp_G	Sp_B	AvDPCM
Lena	0.6088	0.3484	0.2626	0.4066
Pepper	0.5384	0.2914	0.1905	0.3401
Girl	0.5711	0.3782	0.2283	0.3925
House	0.4630	0.3148	0.2136	0.3305

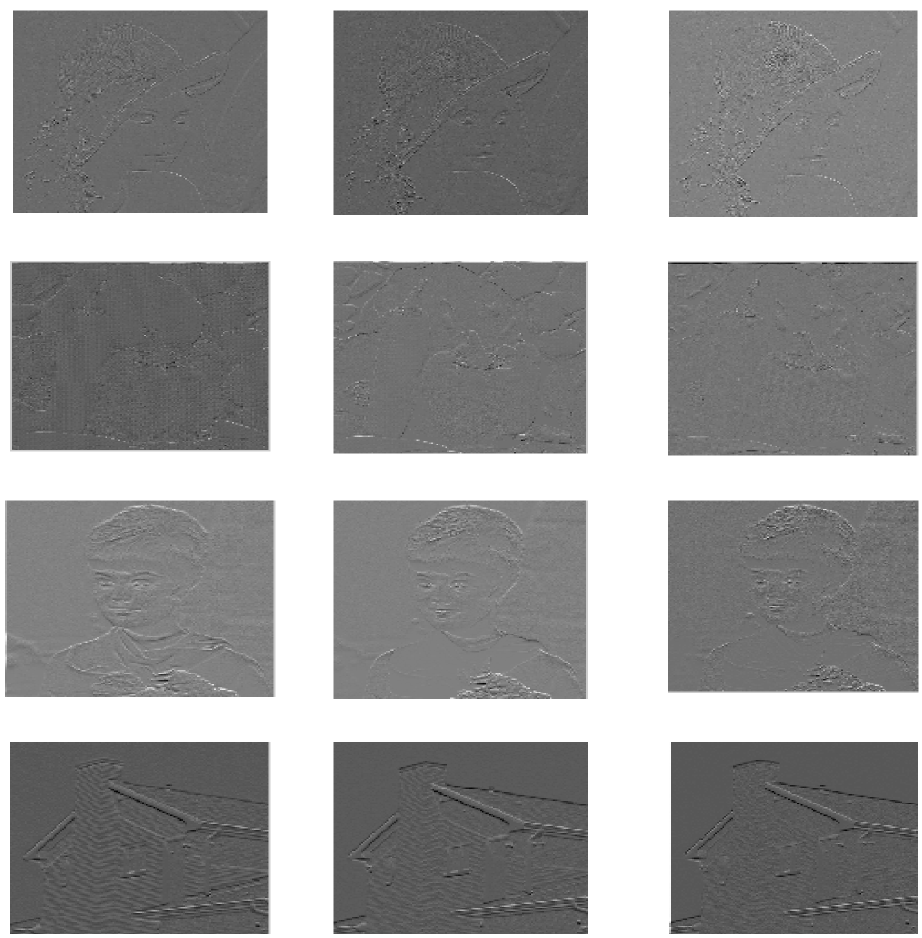

Figure 4. The DPCM of red, green, and blue color bands of the tested images

Table (4) shows the quadtree partitioning scheme of the tested images using different partition control parameters with factor values ($Factor_1$ and $Factor_2$) of two values – (70,30) and (30,70) – where the number of the partitioning segments utilized is an indicator to measure the segmentation process. The number of segments is directly affected by the mentioned parameters along the image details (characteristics). Figure (5) provides an example of the quadtree partitioning scheme using different factors and control parameters. Table (5) demonstrates the time required for the quadtree segmentation process for the test images, using two cases: maximum number (M_{xb}) of blocks and minimum number (M_{nb}) of blocks. The results show the efficiency in partitioning time, which raises the challenge of incorporating it into standard commercial applications as an alternative to the fixed partitioning schemes adopted currently.

Table 3. The computed spatial and spectral threshold values for the tested images

Tested image	$Factor_1$	$Factor_2$	Thr_{Spr}	Thr_{Spl}
Lena	70	30	61	12
	80	20	70	8
	50	50	44	20
	30	70	26	28
	20	80	18	33
Pepper	70	30	35	10
	80	20	40	7
	50	50	25	17
	30	70	15	24
	20	80	10	27
Girl	70	30	55	12
	80	20	63	8
	50	50	39	20
	30	70	24	27
	20	80	16	31
House	70	30	48	10
	80	20	55	7
	50	50	34	17
	30	70	21	23
	20	80	14	26

Table 5. The partitioning time using case1 of able (4) for the tested images

Tested image	Maximum and minimum block size (M_{xb}, M_{nb})	No. Block	Time(Sec)
Lena	(8,2)	34186	35.0343
	(32,8)	2337	1.0060
Pepper	(8,2)	30181	26.7538
	(32,8)	2283	0.7472
Girl	(8,2)	15538	9.0245
	(32,8)	409	0.0156
House	(8,2)	13873	7.3989
	(32,8)	441	0.0249

Table 4. Quadtree partitioning scheme for the tested images

Partitioning control parameters		Case1			
		Lena test image	Pepper test image	Girl test image	House test image
		$Factor_1$=70 $Facto_2$=30 Thr_{spr}=61 Thr_{spl}=12	$Factor_1$=70 $Facto_2$=30 Thr_{spr}=35 Thr_{spl}=10	$Factor_1$=70 $Facto_2$=30 Thr_{spr}=55 Thr_{spl}=12	$Factor_1$=70 $Facto_2$=30 Thr_{spr}=48 Thrspl=10
M_{xb}	M_{nb}	No. blocks (segments)	No. blocks (segments)	No. blocks (segments)	No. blocks (segments)
8	2	34186	30181	15538	13873
8	4	10691	8818	3994	3652
16	2	2911	2788	1294	1720
16	4	2748	2764	1047	1175
32	2	2691	2580	945	812
32	4	2570	2464	761	564
32	8	2337	2283	409	441
		Case2			
Partitioning control parameters		Lena test image	Pepper test image	Girl test image	House test image
		$Factor_1$=30 $Facto_2$=70 Thr_{spr}=26 Thr_{spl}=28	$Factor_1$=70 $Facto_2$=30 Thr_{spr}=15 Thr_{spl}=24	$Factor_1$=70 $Facto_2$=30 Thr_{spr}=24 Thr_{spl}=27	$Factor_1$=70 $Facto_2$=30 Thr_{spr}=21 Thr_{spl}=23
M_{xb}	M_{nb}	No. blocks (segments)	No. blocks (segments)	No. blocks (segments)	No. blocks (segments)
8	2	36757	31753	13078	15211
8	4	11568	9223	3376	3880
16	2	3193	3864	2305	2533
16	4	2882	3121	1464	1816
32	2	2734	2743	1176	1154
32	4	2677	2527	861	918
32	8	2595	2410	667	797

(M_{xb} =16, M_{nb}=2)
($Factor_1$=80, $Factor_2$=20)
No. Blocks= 33253
Time (sec)=31.9487

(M_{xb} =16, M_{nb}=2)
($Factor_1$=40, $Factor_2$=60)
No. Blocks= 9289
Time (sec)= 6.0293

(M_{xb} =16, M_{nb}=4)
($Factor_1$=10, $Factor_2$=90)
No. Blocks= 2755
Time (sec)= 1.9357

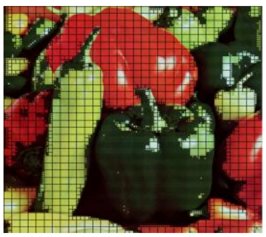

(M_{xb} =16, M_{nb}=2)
($Factor_1$=80, $Factor_2$=20)
No. Blocks= 29086
Time (sec)= 26.0003

(M_{xb} =16, M_{nb}=2)
($Factor_1$=40, $Factor_2$=60)
No. Blocks= 8359
Time (sec)= 4.4677

(M_{xb} =16, M_{nb}=4)
($Factor_1$=10, $Factor_2$=90)
No. Blocks= 2527
Time (sec)= 1.3109

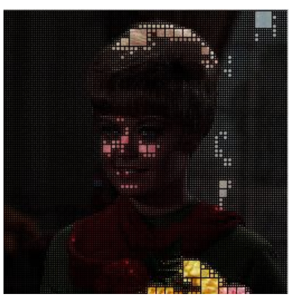

(M_{xb} =16, M_{nb}=2)
($Factor_1$=10, $Factor_2$=90)
No. Blocks= 15496
Time (sec)= 8.9125

(M_{xb} =16, M_{nb}=2)
($Factor_1$=50, $Factor_2$=50)
No. Blocks= 3523
Time (sec)= 2.4844

(M_{xb} =16, M_{nb}=2)
($Factor_1$=75, $Factor_2$=25)
No. Blocks= 661
Time (sec)= 0.1714

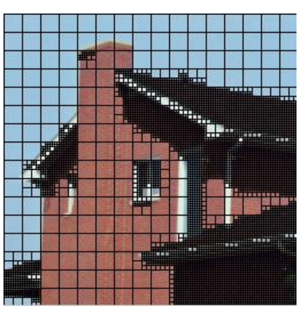

(M_{xb} =16, M_{nb}=2)
($Factor_1$=55, $Factor_2$=45)
No. Blocks= 5989
Time (sec)= 3.9896

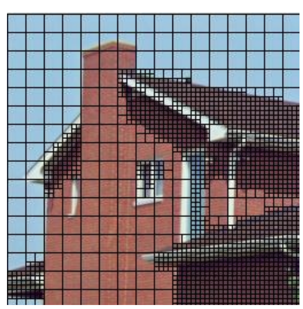

(M_{xb} =16, M_{nb}=2)
($Factor_1$=10, $Factor_2$=90)
No. Blocks= 1612
Time (sec)= 0.2112

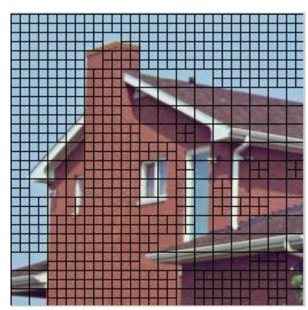

(M_{xb} =16, M_{nb}=4)
($Factor_1$=80, $Factor_2$=20)
No. Blocks= 718
Time (sec)= 0.1932

Figure 5. Quadtree example of the tested images

5. Conclusion

1. The tested segmented images vary in their details, which means that the same image has both complex regions and simple, smooth regions.
2. The proposed technique utilized the spatial and spectral information efficiently, in which the thresholds were generated automatically, along with the need to select the partitioning control parameters of maximum and minimum block size.
3. The segmentation process time is fast, which makes its potential use a challenge to standard techniques such as JPEG.

That said, we must mention the main obstacles related to the proposed system and its use in real applications. It requires an optimization technique to choose the contribution of the spatial and spectral factors, alongside the choosing of effective partitioning control parameters.

References

[1] Y. Q. Shi and H. Sun. Image and Video Compression for Multimedia Engineering, CRC Press: London, 2000.
[2] T. Seemann. Digital Image Processing using Local Segmentation, Ph.D. Thesis, Monash University, Australia, 2002.
[3] M. M. Salem. Multiresolution Image Segmentation. Ph.D. Thesis, Humboldt-Universität zu Berlin, 2008.
[4] R. C. Gonzalez and R. E. Woods. Digital Image Processing,4th edn. Pearson, 2017.
[5] R. Nikhil Pal and K. Sankar Pal, "A Review on Image Segmentation Techniques", *Pattern Recognition*, vol. 26, no. 9, pp. 1277-1294, 1993.
[6] M. Ghanbari. Video Coding an Introduction to Standard Codecs, Institution of Electrical Engineers: London, 1999.
[7] Y. J. Zhang. "An Overview of Image and Video Segmentation in the Last 40 Years", in *Proceedings of the 6th International Symposium on Signal Processing and Its Applications*, 144-151, 2001
[8] H. C. Yang. Scene-Change Detection for MPEG-2 Video Encoder, MSc. Thesis, National Cheng-Kung University, Taiwan, 2002.
[9] W. X. Kang, Q. Q. Yang and R. R. Liang, "The Comparative Research on Image Segmentation Algorithms", in *IEEE Conference on Education Technology and Computer Science (ETCS)*, 703-707, 2009.
[10] T. Shraddha, K. Krishna, B. K. Singh and R. P. Singh, "Image Segmentation: A Review", *International Journal of Computer Science and Management Research*, vol. 1, no. 4, pp. 838-843, 2012.
[11] M. Z. Nida and J. A. Musbah, "Survey on Image Segmentation Techniques". in *International Conference on Communication, Management and Information Technology (ICCMIT 2015), Procedia Computer Science*, 65, 797 – 806, 2015.
[12] Y. Aamir and A. Suhasini, "A Review on Image Segmentation Techniques", *Journal of Applied Science and Computations*, vol. VI, no. I, pp. 3157-3166, 2019.
[13] Y. Fisher. Fractal Image Compression: Theory and Application, Springier Verlage: New York, 1994.
[14] Y. Fisher and S. Menlove. Fractal Image Encoding with HV Partitioning, in Fractal Image Compression: Theory and Application: Springier-Verlage, New York, 1994.
[15] D. Suape, "Fractal Image Compression via Nearest Neighbour Search", in *Conference proceeding of. NATO ASI (North Atlantic Treaty Organization - Advanced Studies Institute) Fractal Image Encoding and Analysis, Fisher, Y.(ed.), Springier Verlage, New York*, 1-23, 1996.

[16] H. Hartenstein, M. Ruhl and D.Saupe, "Region-Based Fractal Image Compression", *IEEE Transactions on Image Processing*, vol. 9, no.7, pp. 1171-1184, 2000.

[17] H. S. Jamila. Fractal Image Compression, Ph.D. Thesis, college of science, University of Baghdad, Iraq, 2001.

[18] K. Ghada. Adaptive Fractal Image Compression, MSc. Thesis, National Computer Center/Higher Education Institute of Computer and Informatic, Baghdad, Iraq, 2001.

[19] B. Kamel and K. Janusz, "Fractal Image Compression with Region-Based Functionality", *IEEE Transactions on Image Processing*, vol. 11, no. 4, pp. 351-362, 2002.

[20] G. Amol, and S. Pawale, "Efficient Domain Search for Fractal Image Compression using Feature Extraction Technique", *Advances in Computer Science Engineering and Applications*, *Springer*, pp. 353-365, 2012.

[21] K. Muhammad, I. Amna, and N. Muhammd, "A Novel Domain Optimization Technique in Fractal Image Compression", in *IEEE Proceedings of World Congress on Intelligent Control and Automation*, 994-999, 2010.

[22] E. Loay and A. Eman, "Speeding-Up Fractal Color Image Compression using Moments Features Based on Symmetry Predictor", in *IEEE International Conference on Information Technology: New Generations*, 508-513, 2011.

[23] L. Shiping and X. Lei, "Non-search Fractal Image Compression Algorithm Research", in *IEEE Chinese Control and Decision Conference (CCDC)*, 4387-4391, 2014.

[24] S. Hanan, "The Quadtree and Related Hierarchical Data Structures", *Computing Surveys*, vol. 16, no. 2, pp.187-260, 1984.

[25] Al-K. Ghadah, "Image Compression based on Quadtree and Polynomial", *International Journal of Computer Applications*, vol. 76, no. 3, pp. 31-37, 2013.

[26] R. Zainab, "Boundary & Geometric Region Features Image Segmentation for Quadtree Partitioning Scheme", *International Journal of Advanced Research in Computer Science and Software Engineering*, vol. 3, no. 12, pp. 778-783, 2013.

[27] K. Qaswaa and Al-M. Haider, "Modelling Based For Segmentation of Quadtree Partitioning Scheme", *International Journal of Advanced Research in Computer Science and Software Engineering*, vol. 4, no. 12, pp. 19-22, 2014.

[28] Al-K. Ghadah, Al-M. Haider and I. Rafaa, "Quadtree Partitioning Scheme using Fixed Predictor Base", *International Journal of Modern Trends in Engineering and Research*, vol. 5, no. 9, pp.1-6, 2018.

[29] M. Detlev, S. Heiko, B. Sebastian, B. Benjamin, H. Philipp, H. Tobias, K. Heiner, L Haricharan,. N. Tung, O. Simon, S. Mischa, S. Karsten, W. Martin and W. Thomas, "Video Compression using Nested Quadtree Structures, Leaf Merging, and Improved Techniques for Motion Representation and Entropy Coding", *IEEE Transactions on Circuits and Systems for Video Technology*, vol. 20, no. 12, pp. 1676-1687, 2012.

[30] W. Zhao, W. Shiqi, Z. Jian, W. Shanshe and M. Siwei, "Effective Quadtree Plus Binary Tree Block Partition Decision for Future Video Coding", in *Proceedings of the IEEE Conferences 2017 Data Compression Conference (DCC) , Snowbird, UT, USA*, 23 – 32, 2017.

[31] K. Ghada, and K. Luay, "Merge Operation Effect on Image Compression Using Fractal Technique", *Um-Salama Science Journal*, vol. 4, no. 1, pp.169-173, 2007.

[32] H. Philipp, O. Simon, B. Benjamin, O. Detlev, B. Kemal, U. Joel, J. C. Gordon and W. Thomas, "Block Merging for Quadtree-Based Partitioning in HEVC", *IEEE Transactions on Circuits and System for Video Technology*, vol. 22, no. 12, pp. 1720-1731, 2012.

[33] S. Rafik, S. Clément, P. François, B. Marie and D. Olivier, "Fast Pseudo-Semantic Segmentation for Joint Region-Based Hierarchical and Multiresolution Representation", in *preceding volume 8305, SPIE Electronic Imaging - Visual Communications and Image Processing, San Francisco, United States*.1-8, 2012.

[34] H. Chim, and Y. Kai, "A Binary Partitioning Approach to Image Compression using Weighted Finite Automata for Large Images", Computer and Mathematics with Applications, vol. 51, no. 11, pp. 1705-1714, 2006.

[35] B. Francesco, F. Filippo, S. Domenico and S. Cristina, "A Quad-Tree Based Multiresolution Approach for Two-dimensional Summary Data", in Proceedings of the 15th International Conference on Scientific and Statistical Database Management (SSDBM), 127-140, 2003.

[36] I. Al Barazanchi and H. R. Abdulshaheed, "Adaptive Illumination Normalization Framework based on Decrease Light Effect for Face Recognition," *Jour Adv Res. Dyn. Control Syst.*, vol. 11, no. 01, pp. 1741–1747, 2019.

[37] N. J. Qasim and I. Barazanchi, "Unconstrained Joint Face Detection and Recognition in Video Surveillance System," Jour Adv Res. Dyn. Control Syst., vol. 11, no. 1, pp. 1855–1862, 2019.

[38] A. S. Abdullah, M. A. Abed, and I. Al Barazanchi, "Improving face recognition by elman neural network using curvelet transform and HSI color space," Period. Eng. Nat. Sci., vol. 7, no. 2, pp. 430–437, 2019.

[39] C. Christopoulos, A. Skodras and T. Ebrahimi, "The JPEG2000 Still Image XOSING System: an Overview", IEEE Transactions on Consumer Electronics, vol. 46, no. 4, pp. 1103-1127, 2000.